Journal of Sound and Vibration (2002) **254**(2), 245–267
doi:10.1006/jsvi.2001.4093, available online at http://www.idealibrary.com on IDEAL®

STOCHASTIC AVERAGING OF STRONGLY NON-LINEAR OSCILLATORS UNDER BOUNDED NOISE EXCITATION

Z. L. HUANG AND W. Q. ZHU

Department of Mechanics, Zhejiang University, Hangzhou 310027, *People's Republic of China. E-mails: huangzhilong@yahoo.com; wqzhu@yahoo.com*

AND

Y. Q. NI AND J. M. KO

Department of Civil and Structural Engineering, The Hong Kong Polytechnic University, Kowloon, Hong Kong. E-mails: ceyqni@polyu.edu.hk; cejmko@polyu.edu.hk

(*Received* 21 *May* 2001, *and in final form* 16 *August* 2001)

A stochastic averaging method for strongly non-linear oscillators under external and/or parametric excitation of bounded noise is proposed by using the so-called generalized harmonics functions. The method is then applied to study the primary resonance of Duffing oscillator with hardening spring under external excitation of bounded noise. The stochastic jump and its bifurcation of the system are observed and explained by using the stationary probability density of amplitude and phase. Subsequently, the method is applied to study the dynamical instability and parametric resonance of Duffing oscillator with hardening spring under parametric excitation of bounded noise. The primary unstable region is delineated by evaluating the Lyapunov exponent of linearized system, and the response and jump of non-linear system around the unstable region are examined by using the sample functions and stationary probability density of amplitude and phase.

1. INTRODUCTION

The response of strongly non-linear oscillators to Gaussian white noise or wide-band random process has been extensively studied by using several techniques such as the stochastic averaging and statistical linearization (see references [1–3] and the references therein). Comparatively, the response of strongly non-linear oscillators to narrow-band random excitation is more complicated and has been less studied. For example, stochastic jump may occur in the Duffing oscillator with hardening spring in the case of external excitation of narrow-band random process and dynamical instability and parametric resonance in the case of parametric excitation. Although the stochastic jump phenomenon of Duffing oscillator under narrow-band excitation has been studied by using several techniques since Lyon *et al.* first observed it in 1961 [4], no one analytical technique can be used to explain the phenomenon satisfactorily [5]. To the authors' knowledge, the parametric resonance of Duffing oscillator under narrow-band random excitation has not been investigated.

Currently, there are two kinds of models for narrow-band random excitation. One is the response of second order linear filter to Gaussian white noise. The other is the so-called

0022-460X/02/$35.00

bounded noise. The latter is a harmonic function with constant amplitude and stochastic frequency and phase. This model was first proposed by Stratonovich [6] and has been used by several researchers in studying the stochastic stability of linear parametric systems [7–9] and chaotic motion of Duffing oscillator with negative linear stiffness [10].

In the present paper, a stochastic averaging method for strongly non-linear oscillators under external and/or parametric excitation of bounded noise is proposed. The method is applied to study the response of Duffing oscillator with hardening spring under external and parametric excitation of bounded noise. The results obtained by using the stochastic averaging method are verified by using digital simulation. The behaviour of the response is examined in detail.

2. THE STOCHASTIC AVERAGING METHOD

The stochastic averaging method for strongly non-linear oscillators subject to external and/or parametric excitations of Gaussian white noise, wide-band random processes, and combined Gaussian white noise and harmonic function, respectively, has been developed (see references [1, 2, 11] and the references therein). Here the case of bounded noise excitation is addressed. The equation of motion of the system studied is of the form

$$\ddot{X} + g(X) = \varepsilon f(X, \dot{X}) + \varepsilon h(X, \dot{X})\xi(t), \tag{1}$$

where g represents a strongly non-linear restoring force, f represents linear and/or non-linear damping, h denotes the amplitude of excitation, ε is a small parameter, $\xi(t)$ is a bounded noise of the form

$$\xi(t) = \cos(\Omega t + \sigma B(t) + \Delta), \tag{2}$$

where Ω and σ^2 are constants representing centre frequency and strength of frequency perturbation, respectively, $B(t)$ is standard Wiener process and Δ is random phase uniformly distributed in $[0, 2\pi]$. $\xi(t)$ is a stationary random process in a wide sense with spectral density

$$S(\omega) = \frac{\sigma^2}{4\pi} \frac{\omega^2 + \Omega^2 + \sigma^4/4}{(\omega^2 - \Omega^2 - \sigma^4/4)^2 + \sigma^4\omega^2} \tag{3}$$

and auto correlation function

$$R(\tau) = \frac{1}{2} \exp\left(-\frac{\sigma^2}{2}|\tau| \right) \cos \Omega\tau. \tag{4}$$

The bandwidth of process $\xi(\tau)$ depends mainly on parameter σ. It is a narrow-band process when σ is small and a wide-band process when σ is large.

Suppose that the non-linear conservative oscillator

$$\ddot{x} + g(x) = 0 \tag{5}$$

has a family of periodic solutions in domain U of phase plane $(x, \dot{x})$. The periodic solution can be expressed as

$$x(t) = a \cos \varphi(t) + b, \tag{6}$$

$$\dot{x}(t) = -av(a, \varphi) \sin \varphi(t), \tag{7}$$

where

$$\varphi(t) = \tau(t) + \theta, \tag{8}$$

$$v(a, \varphi) = \frac{\mathrm{d}\tau}{\mathrm{d}t} = \sqrt{\frac{2[V(a+b) - V(a\cos\varphi + b)]}{a^2 \sin^2 \varphi}}. \tag{9}$$

a and b are constants related by potential energy

$$V(x) = \int_0^x g(u)\,\mathrm{d}u \tag{10}$$

and the total energy

$$H = \tfrac{1}{2}\dot{x}^2 + V(x) \tag{11}$$

is as follows:

$$V(a+b) = V(-a+b) = H, \tag{12}$$

$\cos\varphi(t)$ and $\sin\varphi(t)$ are the so-called generalized harmonic functions [12]. Obviously, a, $v(a, \varphi)$ and θ are the amplitude, instantaneous frequency and phase, respectively, of the oscillator, and $(b, 0)$ is the equilibrium position in phase plane.

Expanding v^{-1} into Fourier series

$$v^{-1}(a, \varphi) = C_0(a) + \sum_{n=1}^{\infty} C_n(a)\cos n\varphi \tag{13}$$

and then integrating equation (9) with respect to τ yields

$$t = C_0(a)\tau + \sum_{n=1}^{\infty} \frac{1}{n} C_n(a)\sin n\varphi. \tag{14}$$

Letting $\tau = 2\pi$ leads to average period

$$T(a) = 2\pi C_0(a) \tag{15}$$

and average frequency

$$\omega(a) = \frac{1}{C_0(a)} \tag{16}$$

of the oscillator.

Now consider the random vibration of system (1). Suppose that the solution is of the form

$$X(t) = A\cos\Phi(t) + B, \tag{17}$$

$$\dot{X}(t) = -Av(A, \Phi)\sin\Phi(t), \tag{18}$$

where

$$\Phi(t) = \tau(t) + \Theta(t), \tag{19}$$

$$v(A, \Phi) = \frac{\mathrm{d}\tau}{\mathrm{d}t} = \sqrt{\frac{2[V(A+B) - V(A\cos\Phi + B)]}{A^2 \sin^2 \Phi}} \tag{20}$$

and A, B, Φ, Θ, τ, v are all random processes. Differentiating equation (17) with respect to t and equating the resultant to equation (18) yields

$$\dot{A}(\cos\Phi + h) - \dot{\Theta}A\sin\Phi = 0, \tag{21}$$

where

$$\bar{h} = \frac{\mathrm{d}B}{\mathrm{d}A} = \frac{g(-A+B) + g(A+B)}{g(-A+B) - g(A+B)}. \tag{22}$$

Differentiating equation (18) with respect to t and then substituting the resultant into equation (1) leads to

$$\dot{A}\left\{v(A,\Phi)\sin\Phi + A\frac{\partial}{\partial A}[v(A,\Phi)\sin\Phi]\right\} + \dot{\Theta}\frac{\partial}{\partial\Phi}[v(A,\Phi)\sin\Phi]$$

$$= -\varepsilon f(A\cos\Phi + B, -Av(A,\Phi)\sin\Phi) - \varepsilon h(A\cos\Phi + B, -Av(A,\Phi)\sin\Phi)\xi(t). \tag{23}$$

Solving equations (21) and (23), we obtain

$$\frac{\mathrm{d}A}{\mathrm{d}t} = \varepsilon F_1(A,\Phi,\Omega t + \Lambda),$$

$$\frac{\mathrm{d}\Theta}{\mathrm{d}t} = \varepsilon F_2(A,\Phi,\Omega t + \Lambda), \tag{24}$$

where

$$\Lambda = \sigma B(t) + \Delta$$

$$F_1 = -\frac{A}{g(A+B)(1+\bar{h})}[f(A\cos\Phi + B, -Av(A,\Phi)\sin\Phi) + h(A\cos\Phi + B,$$

$$-Av(A,\Phi)\sin\Phi)\cos(\Omega t + \Lambda)]v(A,\Phi)\sin\Phi, \tag{25}$$

$$F_2 = -\frac{1}{g(A+B)(1+\bar{h})}[f(A\cos\Phi + B, -Av(A,\Phi)\sin\Phi) + h(A\cos\Phi + B,$$

$$-Av(A,\Phi)\sin\Phi)\cos(\Omega t + \Lambda)]v(A,\Phi)(\cos\Phi + \bar{h}).$$

Since we are interested in narrow-band excitation and resonant case, it is assumed that σ is small and

$$\frac{\Omega}{\omega(A)} = \frac{q}{p} + \varepsilon\delta, \tag{26}$$

where p and q are relatively prime positive small integers and δ is a detuning parameter. Then, from equations (14) and (26), we obtain

$$\Omega t = \frac{q}{p}\Phi + \varepsilon\delta\tau - \frac{q}{p}\Theta + \Omega\sum_{n=1}^{\infty}\frac{1}{n}C_n(A)\sin n\Phi. \tag{27}$$

Introduce a new variable

$$\Gamma = \varepsilon\delta\tau - \frac{q}{p}\Theta + \Lambda \tag{28}$$

then

$$\Omega t + \Lambda = \Psi + \Gamma, \tag{29}$$

where

$$\Psi = \Psi(A, \Phi) = \frac{q}{p}\Phi + \Omega \sum_{n=1}^{\infty} \frac{1}{n} C_n(A) \sin n\Phi. \tag{30}$$

Regarding equation (28) as a transformation form Θ to Γ, equation (24) is transformed into the following Itô stochastic differential equations:

$$\begin{aligned} \mathrm{d}A &= \varepsilon F_1(A, \Phi, \Psi + \Gamma)\,\mathrm{d}t, \\ \mathrm{d}\Gamma &= \left[\left(\frac{\Omega}{\omega(A)} - \frac{q}{p}\right)v(A, \Phi) - \frac{q}{p}\varepsilon F_2(A, \Phi, \Psi + \Gamma)\right]\mathrm{d}t + \sigma\,\mathrm{d}B(t). \end{aligned} \tag{31}$$

Note that when σ is small, A and Γ are a slowly varying process while Φ is a rapidly varying process. Averaging the right side of equation (31) with respect to Φ, we obtain the following averaged Itô equations:

$$\begin{aligned} \mathrm{d}A &= m_1(A, \Gamma)\,\mathrm{d}t, \\ \mathrm{d}\Gamma &= m_2(A, \Gamma)\,\mathrm{d}t + \sigma\,\mathrm{d}B(t), \end{aligned} \tag{32}$$

where

$$\begin{aligned} m_1(A, \Gamma) &= \langle \varepsilon F_1(A, \Phi, \Psi + \Gamma)\rangle_\Phi, \\ m_2(A, \Gamma) &= \left\langle \left(\frac{\Omega}{\omega(A)} - \frac{q}{p}\right)v(A, \Phi) - \frac{q}{p}\varepsilon F_2(A, \Phi, \Psi + \Gamma)\right\rangle_\Phi. \end{aligned} \tag{33}$$

Thus, (A, Γ) is a two-dimensional diffusion process. Itô equation (32) can be solved numerically [13]. However, in most cases it is more convenient to solve the Fokker–Planck–Kolmogorov (FPK) equation associated with Itô equation (32) to obtain the statistics of the response. The FPK equation for transition probability density $p = p(a, \gamma, t \mid a_0, \gamma_0)$ is of the form

$$\frac{\partial p}{\partial t} = -\frac{\partial}{\partial a}[m_1(a, \gamma)p] - \frac{\partial}{\partial \gamma}[m_2(a, \gamma)p] + \frac{\sigma^2}{2}\frac{\partial^2 p}{\partial \gamma^2} \tag{34}$$

with initial condition

$$p = \delta(a - a_0)\delta(\gamma - \gamma_0), \quad t = 0. \tag{35}$$

The boundary condition with respect to γ is periodic, i.e.,

$$\begin{aligned} p|_{\gamma + 2n\pi} &= p|_\gamma, \\ (\partial p/\partial\gamma)|_{\gamma + 2n\pi} &= (\partial p/\partial\gamma)|_\gamma. \end{aligned} \tag{36}$$

One of the boundary conditions with respect to a is

$$p = \textit{finite} \quad \text{at} \quad a = 0. \tag{37}$$

The other boundary condition with respect to a depends on the behavior of the non-linear oscillator in equation (5). In the simplest case, where all solutions of conservative oscillator (5) in whole phase plane $(x, \dot{x})$ are periodic surrounding $(b, 0)$, the other boundary condition of FPK equation (34) with respect to a is

$$p, \frac{\partial p}{\partial a} \to 0, \quad \text{as } a \to \infty. \tag{38}$$

FPK equation (34) with its initial and boundary conditions can be solved numerically by using, e.g., the path integration method [14].

3. DUFFING OSCILLATOR SUBJECT TO EXTERNAL EXCITATION OF BOUNDED NOISE

As the first application of the stochastic averaging method developed in the last section, we study the response of Duffing oscillator with hardening spring to external excitation of bounded noise. The equation of motion of the system is of the form

$$\ddot{X} + \omega^2 X + \alpha X^3 = -\beta \dot{X} + E \cos(\Omega t + \sigma B(t) + \Delta), \tag{39}$$

where ω is the frequency of degenerated linear oscillator, α is the intensity of non-linearity, β is the coefficient of linear damping, and E is the amplitude of excitation. For the present system, $b = \bar{h} = 0$,

$$V(X) = \omega^2 X^2/2 + \alpha X^4/4,$$

$$v^{-1}(A, \Phi) = [(\omega^2 + 3\alpha A^2/4)(1 + \lambda_0 \cos 2\Phi)]^{1/2} = \sum_{n=0}^{\infty} C_{2n}(A) \cos 2n\Phi, \tag{40}$$

$$\lambda_0 = \alpha A^2/4(\omega^2 + 3\alpha A^2/4).$$

For system (39), we are interested in primary resonance, i.e., $q = p = 1$,

$$\Omega/\omega(A) = 1 + \delta. \tag{41}$$

Let

$$\Gamma = \delta\tau - \Theta + \Lambda. \tag{42}$$

Following the procedure given in equations (17)–(33), we obtain the following averaged Itô equations:

$$\begin{aligned} \mathrm{d}A &= m_1(A, \Gamma)\,\mathrm{d}t, \\ \mathrm{d}\Gamma &= m_2(A, \Gamma)\,\mathrm{d}t + \sigma\,\mathrm{d}B(t), \end{aligned} \tag{43}$$

where

$$m_1 = -\beta A(\omega^2 + 5\alpha A^2/8)/2(\omega^2 + \alpha A^2) + E \sin \Gamma \left\langle v(A, \Phi) \sin \Phi \sin\left(\Phi + \Omega \sum_{n=1}^{\infty} \frac{1}{2n} C_{2n}(A) \sin 2n\Phi\right)\right\rangle_{\Phi} \Big/ (\omega^2 + \alpha A^2)$$

$$m_2 = [\Omega C_0(A) - 1]\langle v(A, \Phi)\rangle_{\Phi} + E \cos \Gamma \left\langle v(A, \Phi) \cos \Phi \times \cos\left(\Phi + \Omega \sum_{n=1}^{\infty} \frac{1}{2n} C_{2n}(A) \sin 2n\Phi\right)\right\rangle_{\Phi} \Big/ A(\omega^2 + \alpha A^2). \tag{44}$$

In the case of deterministic harmonic excitation, $\sigma = \Delta = 0$ and equation (43) is reduced to ordinary differential equations

$$\frac{\mathrm{d}a}{\mathrm{d}t} = m_1(a, \gamma),$$

$$\frac{\mathrm{d}\gamma}{\mathrm{d}t} = m_2(a, \gamma). \tag{45}$$

Solving equation (45) in the case of $\mathrm{d}a/\mathrm{d}t = 0$ and $\mathrm{d}\gamma/\mathrm{d}t = 0$ yields the stationary amplitude response curve of Duffing oscillator under harmonic excitation, as shown in Figure 1.

The FPK equation associated with Itô equation (43) is of the form of equation (34) with m_1 and m_2 defined by equation (44). For system (39), the initial and boundary conditions of

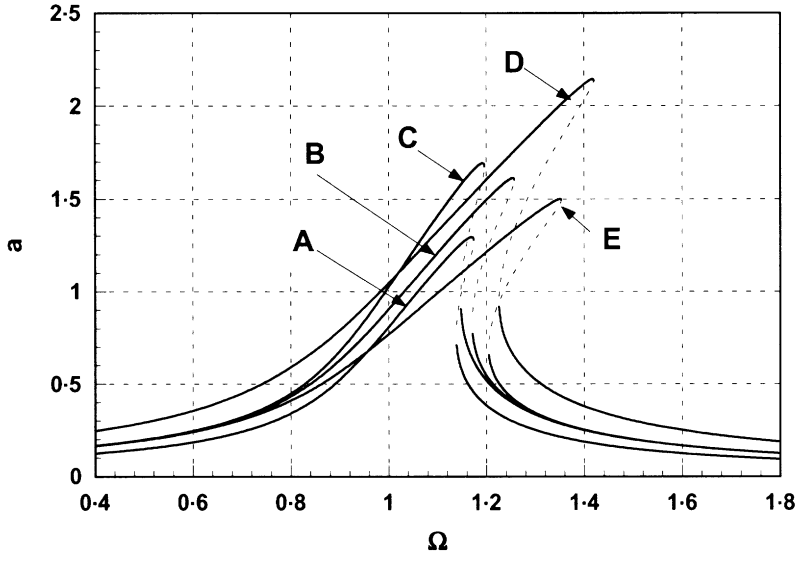

Figure 1. Amplitude response curve of Duffing oscillator under external harmonic excitation, curve A: $\omega = 1{\cdot}0$, $\alpha = 0{\cdot}3$, $\beta = 0{\cdot}1$, $E = 0{\cdot}15$; curve B: $\omega = 1{\cdot}0$, $\alpha = 0{\cdot}3$, $\beta = 0{\cdot}1$, $E = 0{\cdot}20$; curve C: $\omega = 1{\cdot}0$, $\alpha = 0{\cdot}2$, $\beta = 0{\cdot}1$, $E = 0{\cdot}20$; curve D: $\omega = 1{\cdot}0$, $\alpha = 0{\cdot}3$, $\beta = 0{\cdot}1$, $E = 0{\cdot}3$; curve E: $\omega = 1{\cdot}0$, $\alpha = 0{\cdot}5$, $\beta = 0{\cdot}1$, $E = 0{\cdot}20$.

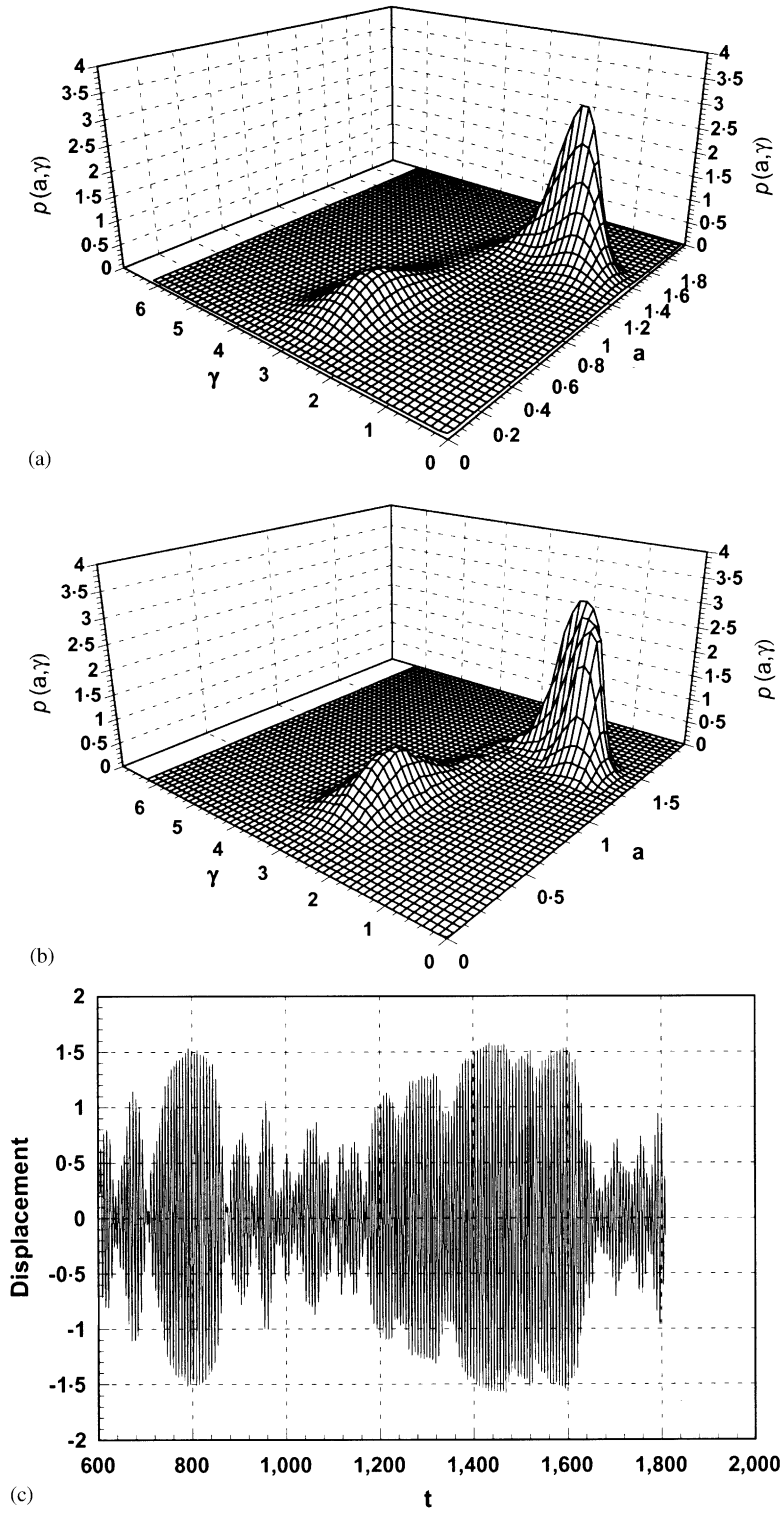

Figure 2. Stationary probability density $p(a, \gamma)$ and sample functions of displacement of system (39), $\alpha = 0{\cdot}3$, $\beta = 0{\cdot}1$, $\omega = 1{\cdot}0$, $\Omega = 1{\cdot}2$, $E = 0{\cdot}2$, $\sigma^2 = 0{\cdot}02$. (a) $p(a, \gamma)$ by the stochastic averaging and path integration; (b) $p(a, \gamma)$ from the digital simulation of equation (39); (c) sample function of displacement from digital simulation.

the FPK equation are of the form of equations (35)–(38). Using the method of path integration [14], we obtain the stationary joint probability density $p(a, \gamma)$ of amplitude and phase. One such density is shown in Figure 2(a). To confirm the result obtained by using the stochastic averaging and path integration, a similar result obtained from digital simulation is shown in Figure 2(b). It is seen that the two results are in excellent agreement.

The stationary joint probability density in Figure 2 is bimodal, which implies that the system has two more probable motions. Based on our experience in the study of the response of Duffing oscillator with hardening spring to narrow-band excitation [5] and to combined white noise and harmonic excitations [11], it is expected that stochastic jumps may occur between the two more probable motions. The time history of displacement shown in Figure 2(c) verifies our inference. This fact further confirms that the stochastic jump is essentially the transition of the response from one more probable motion to another or *vice versa* [5, 11].

A major difference between the stochastic and deterministic jumps of Duffing oscillator with hardening spring is that the latter occurs only at the two extremes of the frequency interval of triple-valued amplitude solution while the former may happen at any frequency

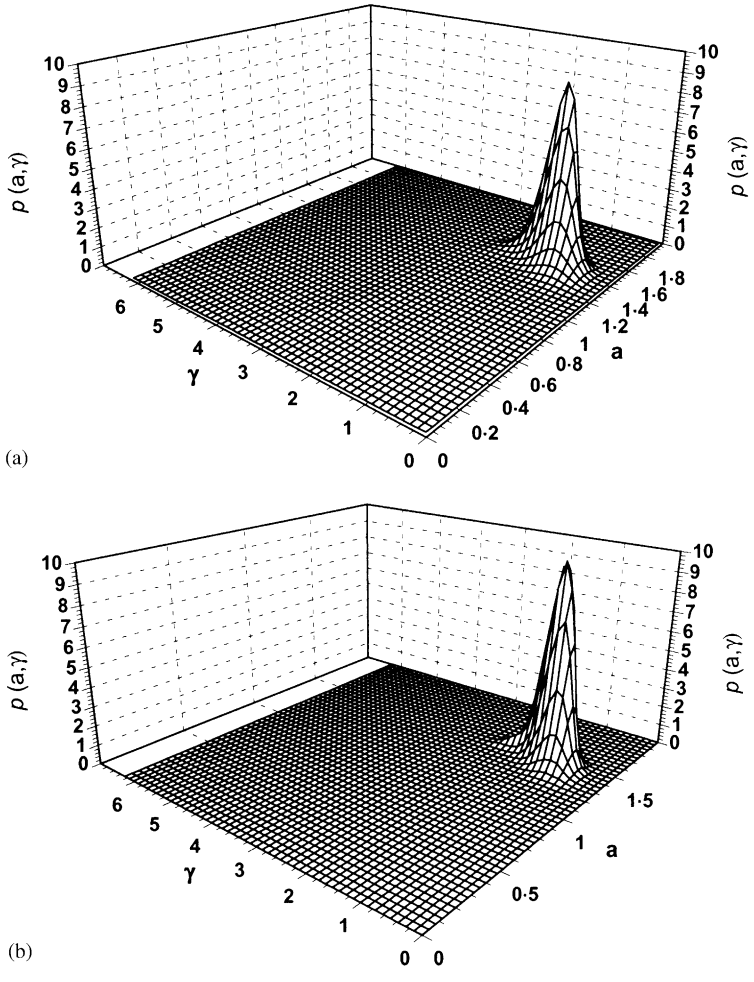

Figure 3. Stationary probability density $p(a, \gamma)$ of system (39), $\alpha = 0{\cdot}3$, $\beta = 0{\cdot}1$, $\omega = 1{\cdot}0$, $\Omega = 1{\cdot}2$, $E = 0{\cdot}2$, $\sigma^2 = 0{\cdot}01$: (a) by the stochastic averaging and path integration; (b) from the digital simulation of equation (39).

of the frequency interval. In fact, the stochastic jumps described in Figure 2 occur at $\Omega = 1{\cdot}2$, which is not one of the two extremes of the frequency interval (see curve B in Figure 1). In this case, the stochastic jump happens due to the stochastic perturbation of excitation frequency. Thus, it is expected that the jump will disappear when the intensity of frequency perturbation, σ^2, is small. This inference is verified in Figure 3. On the other hand, it is expected that jumps occur more often when σ^2 is larger. It is shown in Figure 4.

Another major difference between the stochastic and deterministic jumps of Duffing oscillator with hardening spring is that the former happens forward and backward (see Figure 2(c)) while the latter happens only in one direction, i.e., from larger amplitude to smaller on at upper extreme of the frequency interval or from smaller amplitude to larger one at lower extreme of the frequency interval.

As shown in reference [5, 11], whether stochastic jumps occur or not depends on the parameters of the system and excitation, such as intensity of non-linearity, frequency ratio ω/Ω and amplitude of excitation. This phenomenon was called the bifurcation of stochastic jump. For example, comparison of Figures 2, 5 and 6 shows that the stochastic jumps may occur only when the excitation amplitude E takes the value in some subinterval of (0·15, 0·3)

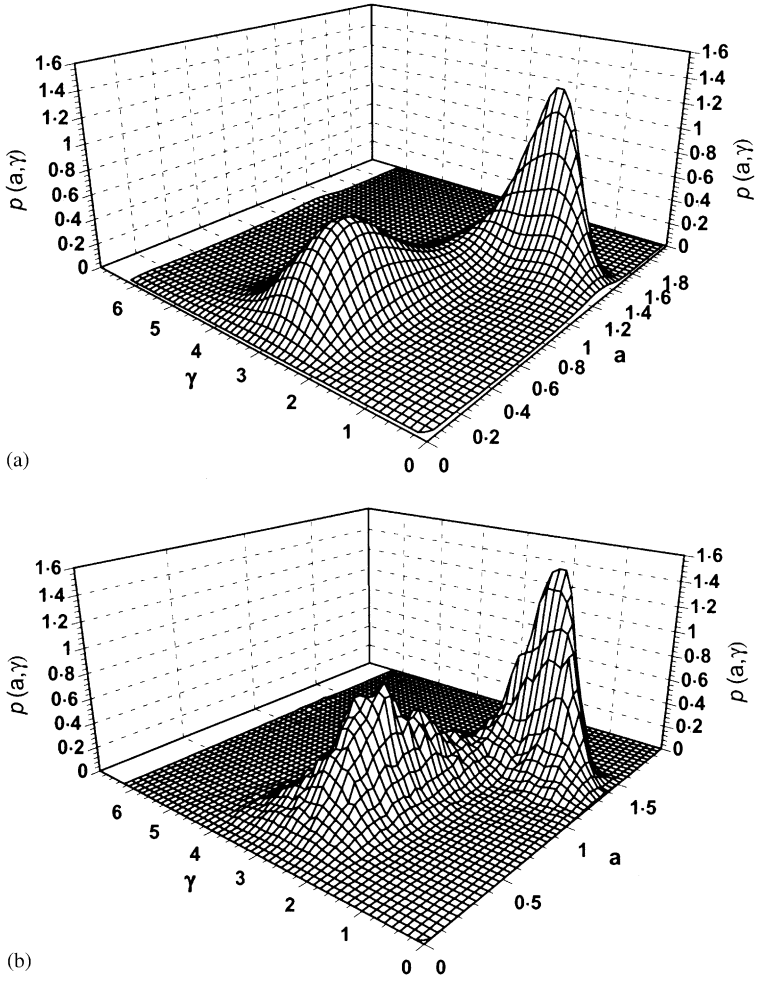

Figure 4. Stationary probability density $p(a, \gamma)$ of system (39), $\alpha = 0{\cdot}3$, $\beta = 0{\cdot}1$, $\omega = 1{\cdot}0$, $\Omega = 1{\cdot}2$, $E = 0{\cdot}2$, $\sigma^2 = 0{\cdot}04$: (a) by the stochastic averaging and path integration; (b) from the digital simulation of equation (39).

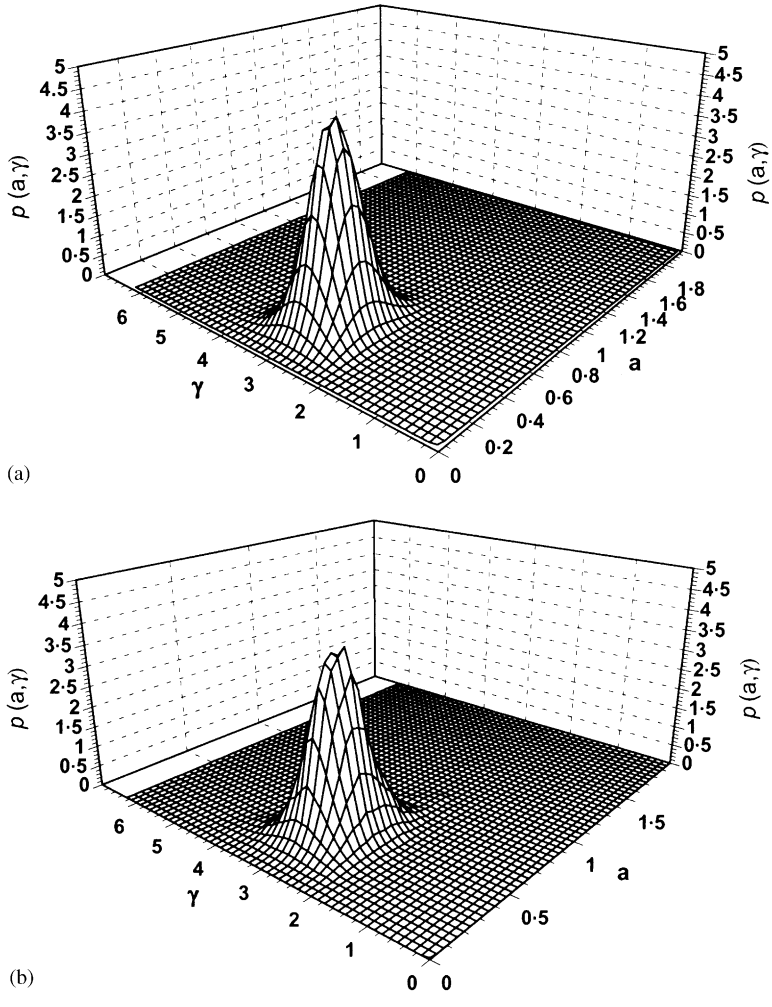

Figure 5. Stationary probability density $p(a, \gamma)$ of system (39), $\alpha = 0{\cdot}3$, $\beta = 0{\cdot}1$, $\omega = 1{\cdot}0$, $\Omega = 1{\cdot}2$, $E = 0{\cdot}15$, $\sigma^2 = 0{\cdot}02$: (a) by the stochastic averaging and path integration; (b) from the digital simulation of equation (39).

provided that the other parameters are kept unchanged. Figures 7 and 8 indicate that the stochastic jump would not occur if the central frequency of the excitation is far outside of the frequency interval of the triple valued amplitude solution (see Figure 1). Comparison of Figures 2, 9 and 10 shows that stochastic jumps may occur only when the intensity of non-linearity, α, is in some subinterval of (0·25, 0·5) provided the other parameters are unchanged.

4. DUFFING OSCILLATOR SUBJECT TO PARAMETRIC EXCITATION OF BOUNDED NOISE

As the second application of the stochastic averaging method proposed in the present paper, now we consider the stability and response of Duffing oscillator under parametric excitation of bounded noise. The equation of motion is of the form

$$\ddot{X} + \omega^2 X + \alpha X^3 = -\beta \dot{X} + EX \cos(\Omega t + \sigma B(t) + \Delta), \tag{46}$$

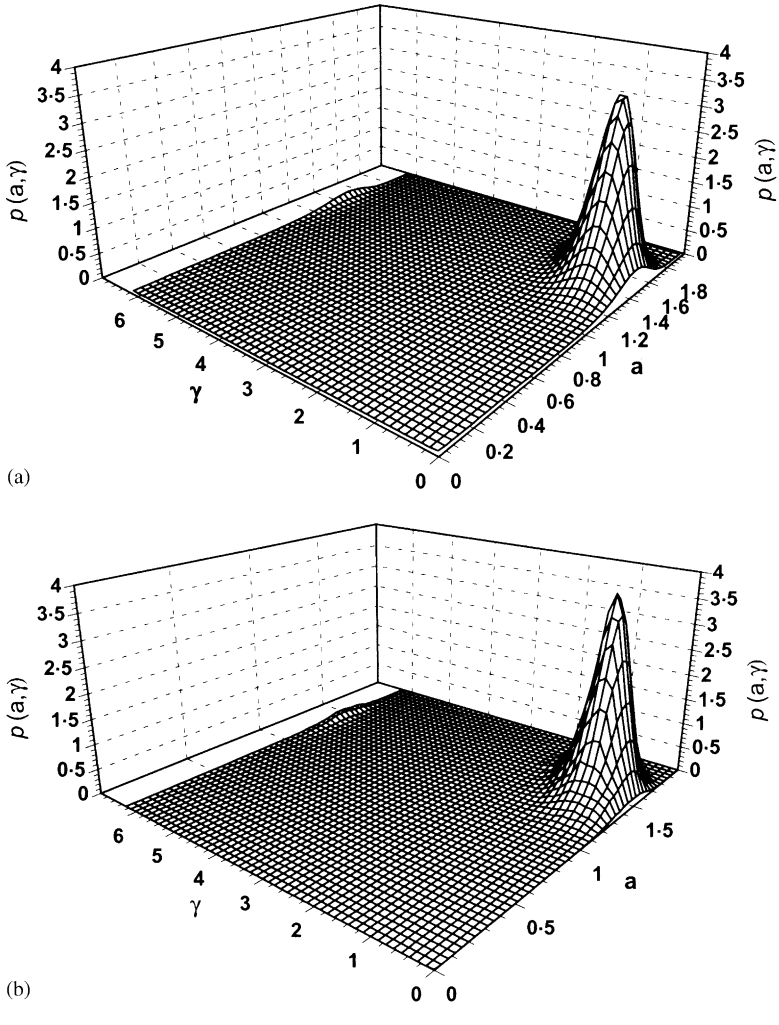

Figure 6. Stationary probability density $p(a, \gamma)$ of system (39), $\alpha = 0{\cdot}3$, $\beta = 0{\cdot}1$, $\omega = 1{\cdot}0$, $\Omega = 1{\cdot}2$, $E = 0{\cdot}3$, $\sigma^2 = 0{\cdot}02$: (a) by the stochastic averaging and path integration; (b) from the digital simulation of equation (39).

where the notations are the same as those in system (39). One practical example of equation (46) is the single-mode model of cables vibration in cable-stayed bridges caused by the parametric excitation of the deck and/or towers in vortex shedding and buffeting [15]. Note that equation (40) holds in this case. However, for the present system, we are interested in the primary parametric resonance, i.e., $q = 2$, $p = 1$,

$$\frac{\Omega}{\omega(A)} = 2 + \delta. \tag{47}$$

Let

$$\Gamma = \delta\tau - 2\Theta + \Lambda. \tag{48}$$

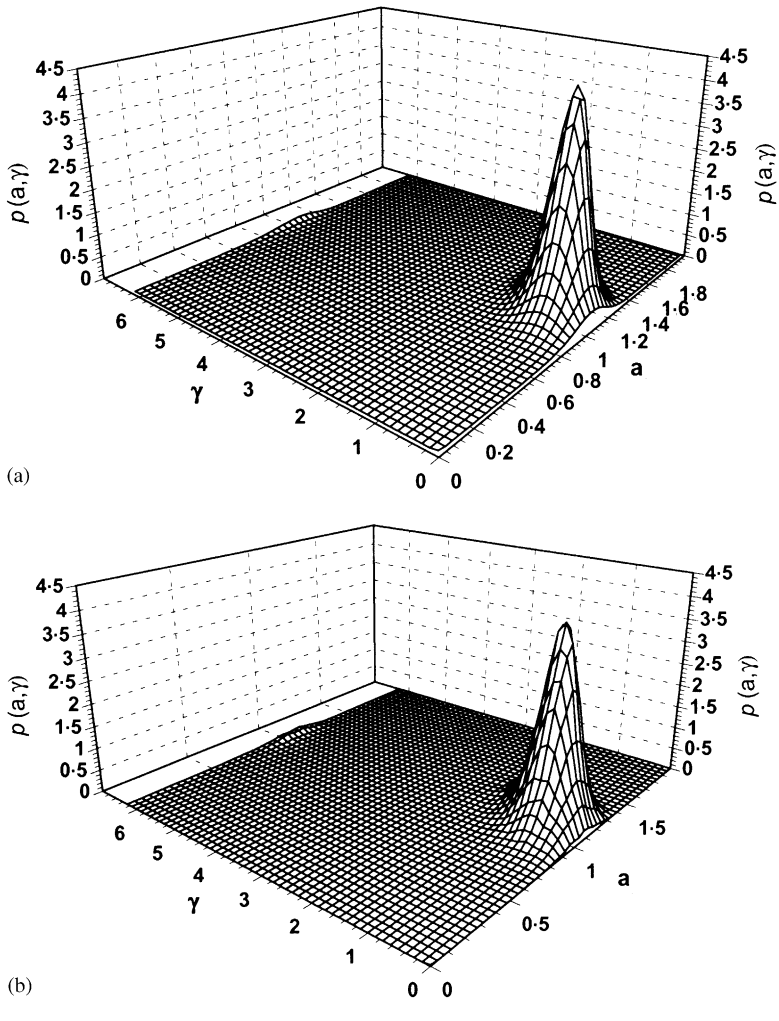

Figure 7. Stationary probability density $p(a, \gamma)$ of system (39), $\alpha = 0{\cdot}3$, $\beta = 0{\cdot}1$, $\omega = 1{\cdot}0$, $\Omega = 1{\cdot}1$, $E = 0{\cdot}2$, $\sigma^2 = 0{\cdot}02$: (a) by the stochastic averaging and path integration; (b) from the digital simulation of equation (39).

Following the procedure given in equations (17)–(33), we obtain the following averaged Itô equations for system (46):

$$\mathrm{d}A = m_1(A, \Gamma)\,\mathrm{d}t, \tag{49}$$

$$\mathrm{d}\Gamma = m_2(A, \Gamma)\,\mathrm{d}t + \sigma\,\mathrm{d}B(t), \tag{50}$$

where

$$m_1 = -\beta A(\omega^2 + 5\alpha A^2/8)/2(\omega^2 + \alpha A^2) + EA\sin\Gamma$$

$$\times \left\langle v(A, \Phi)\sin 2\Phi \sin\left(2\Phi + \Omega \sum_{n=1}^{\infty} \frac{1}{2n} C_{2n}(A)\sin 2n\Phi\right)\right\rangle_{\Phi} \Big/ 2(\omega^2 + \alpha A^2),$$

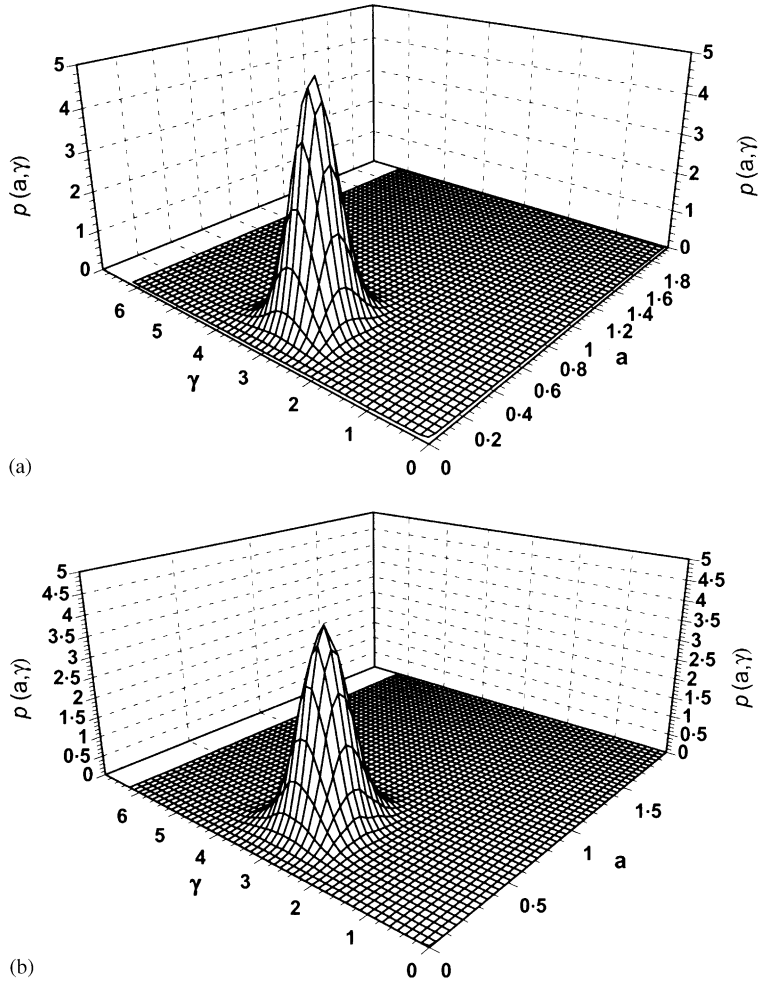

Figure 8. Stationary probability density $p(a, \gamma)$ of system (39), $\alpha = 0{\cdot}3$, $\beta = 0{\cdot}1$, $\omega = 1{\cdot}0$, $\Omega = 1{\cdot}3$, $E = 0{\cdot}2$, $\sigma^2 = 0{\cdot}02$: (a) by the stochastic averaging and path integration; (b) from the digital simulation of equation (39).

$$m_2 = [\Omega C_0(A) - 2]\langle v(A,\ \Phi)\rangle_\Phi + E\cos\Gamma\left\langle v(A,\Phi)\cos 2\Phi\cos\left(2\Phi + \Omega\sum_{n=1}^{\infty}\frac{1}{2n}C_{2n}(A)\sin 2n\Phi\right)\right\rangle_\Phi \Big/ (\omega^2 + \alpha A^2). \tag{51}$$

The instability of system (46) is firstly examined by using its linearized equation. For linearized system ($\alpha = 0$), Itô equations (49) and (50) are reduced to

$$\mathrm{d}A = m_{1l}(A, \Gamma)\,\mathrm{d}t, \tag{52}$$

$$\mathrm{d}\Gamma = m_{2l}(A, \Gamma)\,\mathrm{d}t + \sigma\,\mathrm{d}B(t), \tag{53}$$

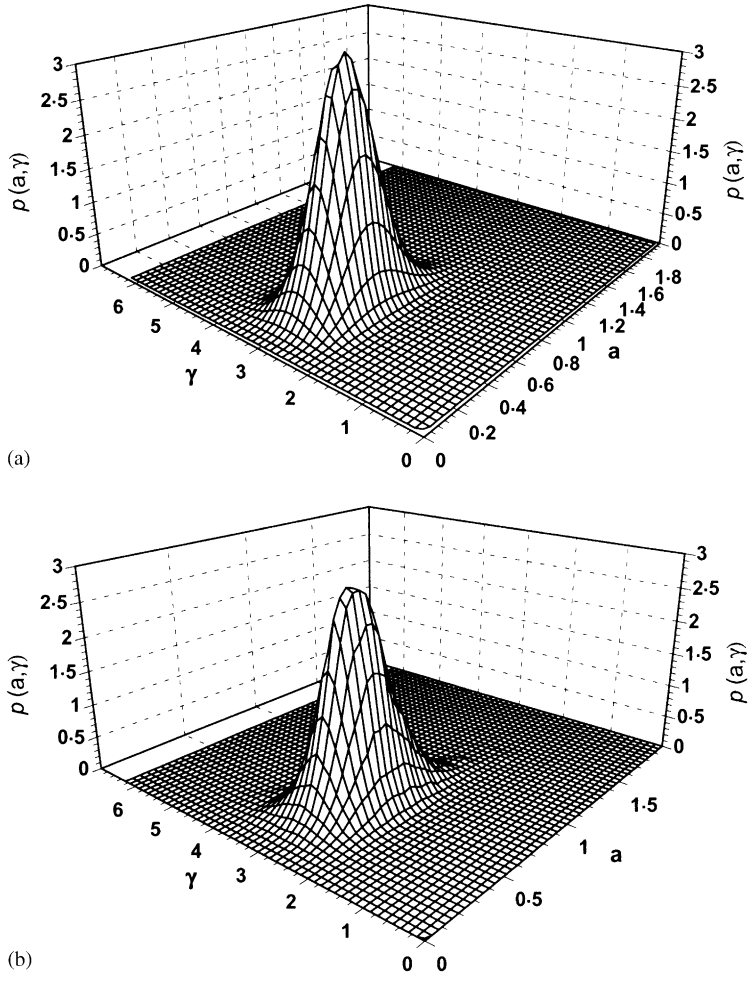

Figure 9. Stationary probability density $p(a, \gamma)$ of system (39), $\alpha = 0{\cdot}2$, $\beta = 0{\cdot}1$, $\omega = 1{\cdot}0$, $\Omega = 1{\cdot}2$, $E = 0{\cdot}2$, $\sigma^2 = 0{\cdot}02$: (a) by the stochastic averaging and path integration; (b) from the digital simulation of equation (39).

where

$$m_{1l} = -\frac{1}{2}\beta A + \frac{EA}{4\omega}\sin\Gamma, \tag{54}$$

$$m_{2l} = (\Omega - 2\omega) + \frac{E}{2\omega}\cos\Gamma. \tag{55}$$

Let

$$\rho = \ln A. \tag{56}$$

The Itô equation for ρ is obtained from equation (52) by using Itô differential rule

$$\mathrm{d}\rho = \left(-\frac{1}{2}\beta + \frac{E}{4\omega}\sin\Gamma\right)\mathrm{d}t. \tag{57}$$

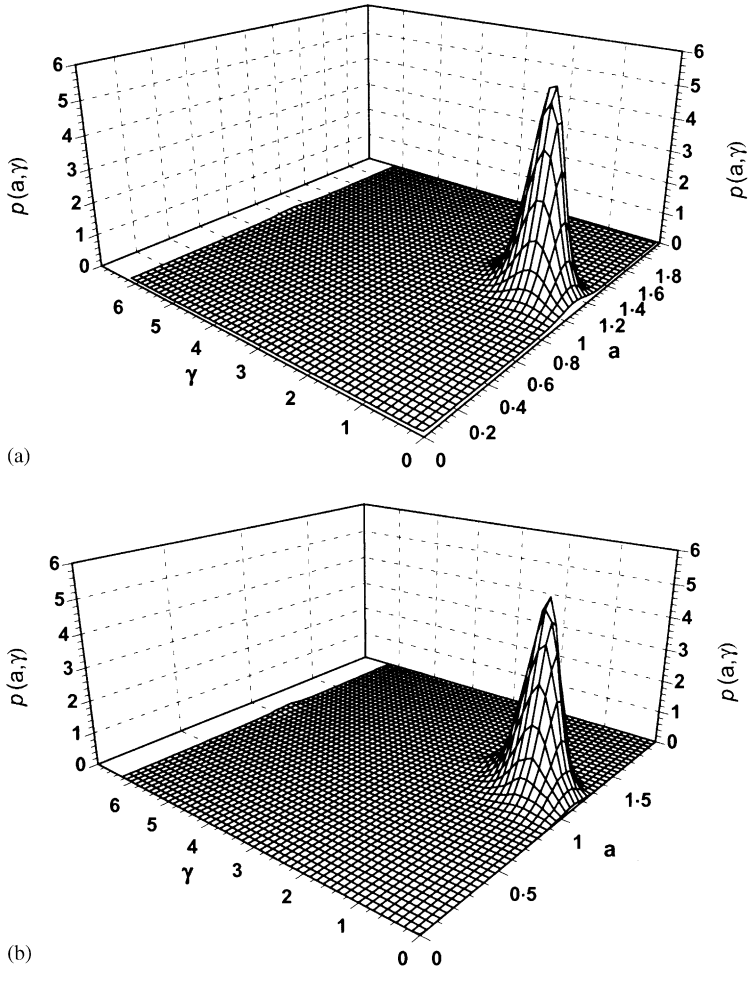

Figure 10. Stationary probability density $p(a, \gamma)$ of system (39), $\alpha = 0{\cdot}5$, $\beta = 0{\cdot}1$, $\omega = 1{\cdot}0$, $\Omega = 1{\cdot}2$, $E = 0{\cdot}2$, $\sigma^2 = 0{\cdot}02$: (a) by the stochastic averaging and path integration; (b) from the digital simulation of equation (39).

The Lyapunov exponent of the linearized system is defined as

$$\lambda = \lim_{t \to \infty} \frac{1}{2t} \ln \left[X^2(t) + \frac{1}{\omega^2} \dot{X}^2(t) \right], \tag{58}$$

which, making use of equations (17) and (18), becomes

$$\lambda = \lim_{t \to \infty} \frac{1}{t} \ln \left(A(t) = \lim_{t \to \infty} \frac{1}{t} \rho(t) \right). \tag{59}$$

The Lyapunov exponent is a measure of the average exponential growth rate of the amplitude process $A(t)$ for large value of t and is a deterministic number with probability one (w.p.1) for the system given by equation (52) or (57). If Lyapunov exponent is negative,

the trivial solution of system (46) will be stable w.p.1. If the Lyapunov exponent is positive, then the trivial solution will be unstable w.p.1.

In order to calculate λ, we integrate both sides of equation (57) to obtain

$$\rho(t) - \rho(0) = -\frac{1}{2}\beta t + \frac{E}{4\omega} + \frac{E}{4\omega}\int_0^t \sin \Gamma(t)\, \mathrm{d}t. \tag{60}$$

Using equation (59), the Lyupunov exponent can be rewritten as

$$\lambda = -\frac{1}{2}\beta + \frac{E}{4\omega}\lim_{t\to\infty}\frac{1}{t}\int_0^t \sin \Gamma(t)\, \mathrm{d}t. \tag{61}$$

The random process $\Gamma(t)$ given by equation (53) can be shown to be ergodic. In this case, we can write

$$\lim_{t\to\infty}\frac{1}{t}\int_0^t \sin \Gamma(t)\, \mathrm{d}t = E[\sin \Gamma] \quad \text{w.p.1}, \tag{62}$$

where $E[\cdot]$ denotes the expectation operator. Thus, w.p.1

$$\lambda = -\frac{1}{2}\beta + \frac{E}{4\omega}E[\sin \Gamma]. \tag{63}$$

To evaluate $E[\sin \Gamma]$, note that $\Gamma(t)$ is a one-dimensional diffusion process governed by Itô equation (53). The stationary probability density $p(\gamma)$ can be obtained from solving the following reduced FPK equation associated with equation (53):

$$\sigma^2\frac{\mathrm{d}^2 p}{\mathrm{d}\gamma^2} - 2\frac{\mathrm{d}}{\mathrm{d}\gamma}\left[\left((\Omega - 2\omega) + \frac{E}{2\omega}\cos\gamma\right)p\right] = 0. \tag{64}$$

The solution to equation (64) satisfying the periodic condition is

$$p(\gamma) = C\exp\left\{\frac{2}{\sigma^2}\left[(\Omega - 2\omega)\gamma + \frac{E}{2\omega}\sin\gamma\right]\right\}$$
$$\times\int_\gamma^{2\pi+\gamma}\exp\left\{\frac{-2}{\sigma^2}\left[(\Omega - 2\omega)\gamma + \frac{E}{2\omega}\sin\gamma\right]\right\}\mathrm{d}\gamma, \tag{65}$$

where C is a normalizing constant. Finally, the Lyapunov exponent is

$$\lambda = -\frac{1}{2}\beta + \frac{E}{4\omega}\int_0^{2\pi}\sin\gamma\, p(\gamma)\, \mathrm{d}\gamma. \tag{66}$$

Letting $\lambda = 0$ yields the boundary of the main unstable region of system (46) in plane (E, Ω_r), where $\Omega_r = 2\omega/\Omega$.

Some numerical results are shown in Figure 11. It is seen that the stochastic perturbation of excitation frequency in general reduces the unstable region. However, at higher level of excitation amplitude, large frequency perturbation may widen the unstable region.

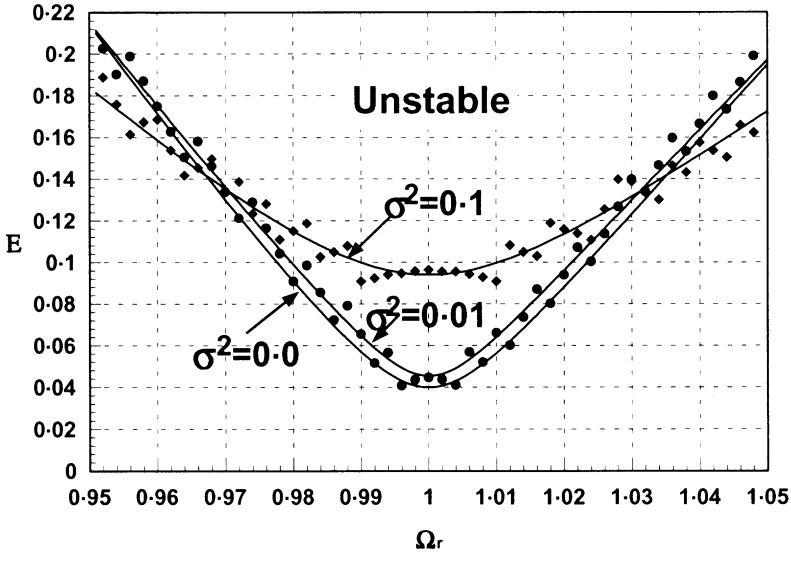

Figure 11. Primary unstable region of system (46). $\omega = 1$, $\alpha = 0$, $\beta = 0{\cdot}02$, $\Omega_r = 2\omega/\Omega$. ——, by letting λ in equation (66) vanish ● ◆, from digital simulation.

Now let us examine the response of system (46) around the unstable region. In the case of harmonic excitation, $\sigma = \Delta = 0$, Itô stochastic differential equation (49) and (50) are reduced to ordinary differential equations

$$\frac{\mathrm{d}a}{\mathrm{d}t} = m_1(a, \gamma), \tag{67}$$

$$\frac{\mathrm{d}\gamma}{\mathrm{d}t} = m_2(a, \gamma). \tag{68}$$

Letting $\mathrm{d}a/\mathrm{d}t = 0$, $\mathrm{d}\gamma/\mathrm{d}t = 0$ in equations (67) and (68), we obtain the stationary amplitude response curve of Duffing oscillator under harmonic parametric excitation

$$\left[\frac{\beta(\omega^2 + 5\alpha a^2/8)}{\left\langle v(a,\varphi)\sin 2\varphi \sin\left(2\varphi + \Omega\sum_{n=1}^{\infty}\frac{1}{2n}C_{2n}(a)\sin 2n\varphi\right)\right\rangle_{\varphi}}\right]^2 + \left[\frac{(\Omega C_0(a) - 2)\langle v(a,\varphi)\rangle_{\varphi}(\omega^2 + \alpha a^2)}{\left\langle v(a,\varphi)\cos 2\varphi \cos\left(2\varphi + \Omega\sum_{n=1}^{\infty}\frac{1}{2n}C_{2n}(a)\sin 2n\varphi\right)\right\rangle_{\varphi}}\right]^2 = E^2. \tag{69}$$

One such curve is shown in Figure 12. For comparison, another response curve obtained by using the multi-scale method is also shown in Figure 12. The later curve is governed by equation [16]

$$a^2 = \frac{4}{3\alpha}\left\{\left[\left(\frac{\Omega}{2}\right)^2 - \omega^2\right] \mp \sqrt{E^2 - \Omega^2\beta^2}\right\}. \tag{70}$$

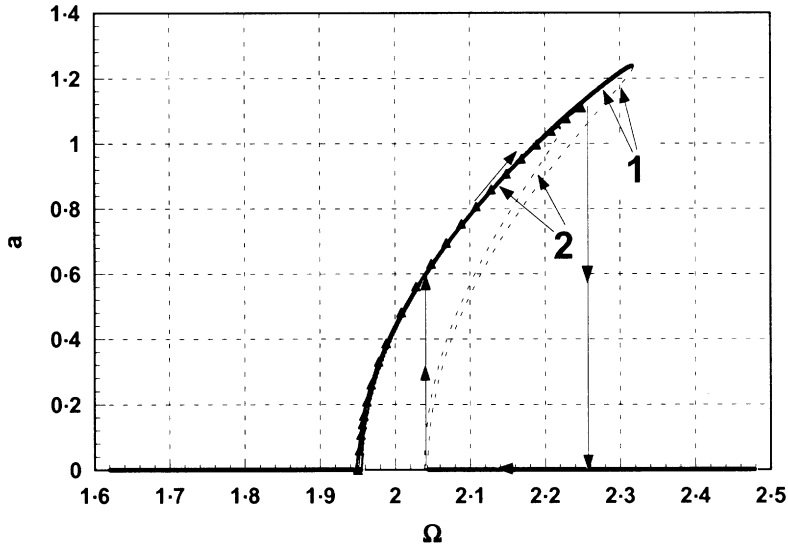

Figure 12. Amplitude response curve of Duffing oscillator under parametric harmonic excitation, $\omega = 1$, $\alpha = 0{\cdot}3$, $E = 0{\cdot}2$, $\beta = 0{\cdot}09$. 1, by the stochastic averaging method; 2, by the multi-scale method; ▲, from the digital simulation.

The two curves are in quite good agreement except that the stochastic averaging method predicts more high-level stable amplitude response. The result from digital simulation indicates that the actual amplitude response curve is somewhere between the two curves given by the stochastic averaging method and multi-scale method. In unstable region, the non-linearity in stiffness limits the divergence of the amplitude due to instability and there is only one non-zero stable amplitude. In a frequency interval on the right-hand side of unstable region, equations (69) and (70) have three solutions, among them two are stable and the other is unstable. So, jumps may occur as shown in Figure 12.

In the case of bounded noise excitation, the stationary response of system (46) is depicted by using stationary joint probability density of amplitude and phase, which can be obtained from solving the reduced FPK equation associated with Itô equations (49) and (50) by using the method of path integration [14]. In unstable region, the trivial solution of system (46) is unstable and there is only one non-zero more probable motion as shown in Figure 13 by the unimodal stationary probability density of amplitude and phase. If the system is initially located around equilibrium position, the response will diverge toward the more probable non-zero motion, see Figure 14. In the frequency interval of triple-valued amplitude solution, there are two more probable motions: one with non-zero amplitude and one with zero amplitude. It is observed that the probable motion with zero amplitude has much stronger attraction so that the final stationary state of the system is at equilibrium position. If the system is initially located at the other probable motion with non-zero amplitude, it will decay and approach the equilibrium position without back jump (see Figure 15(a)). This is because the zero amplitude probable motion has larger attraction domain and the amplitude of excitation is proportional to displacement. The transient period depends on the central frequency Ω and the intensity of frequency perturbation, σ^2. As shown in Figure 15(a)–15(d), the larger Ω or σ^2 is, the sooner the transition is.

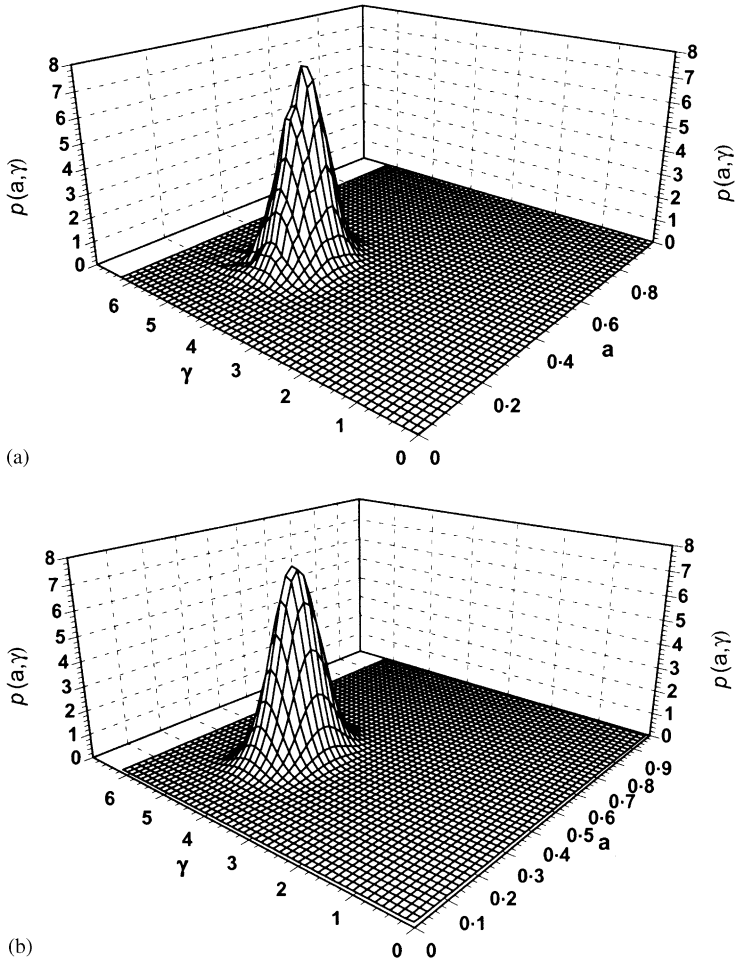

Figure 13. Stationary probability density $p(a, \gamma)$ of system (46), $\alpha = 0{\cdot}3$, $\beta = 0{\cdot}09$, $\omega = 1{\cdot}0$, $\Omega = 2{\cdot}0$, $E = 0{\cdot}2$, $\sigma^2 = 0{\cdot}01$: (a) by the stochastic averaging and path integration; (b) from the digital simulation of equation (46).

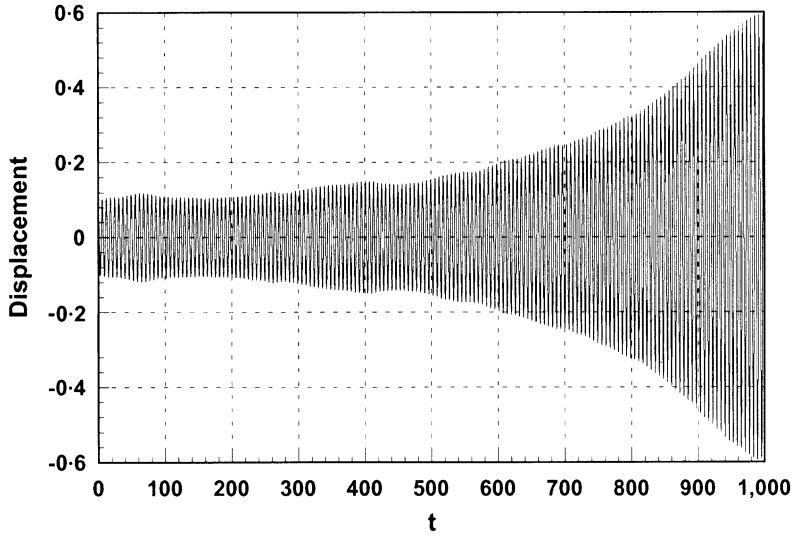

Figure 14. Sample function of displacement of system (46), $\alpha = 0{\cdot}3$, $\beta = 0{\cdot}09$, $\omega = 1{\cdot}0$, $\Omega = 2{\cdot}04$, $E = 0{\cdot}2$, $\sigma^2 = 0{\cdot}01$, $x_0 = 0{\cdot}1$, $\dot{x}_0 = 0{\cdot}0$.

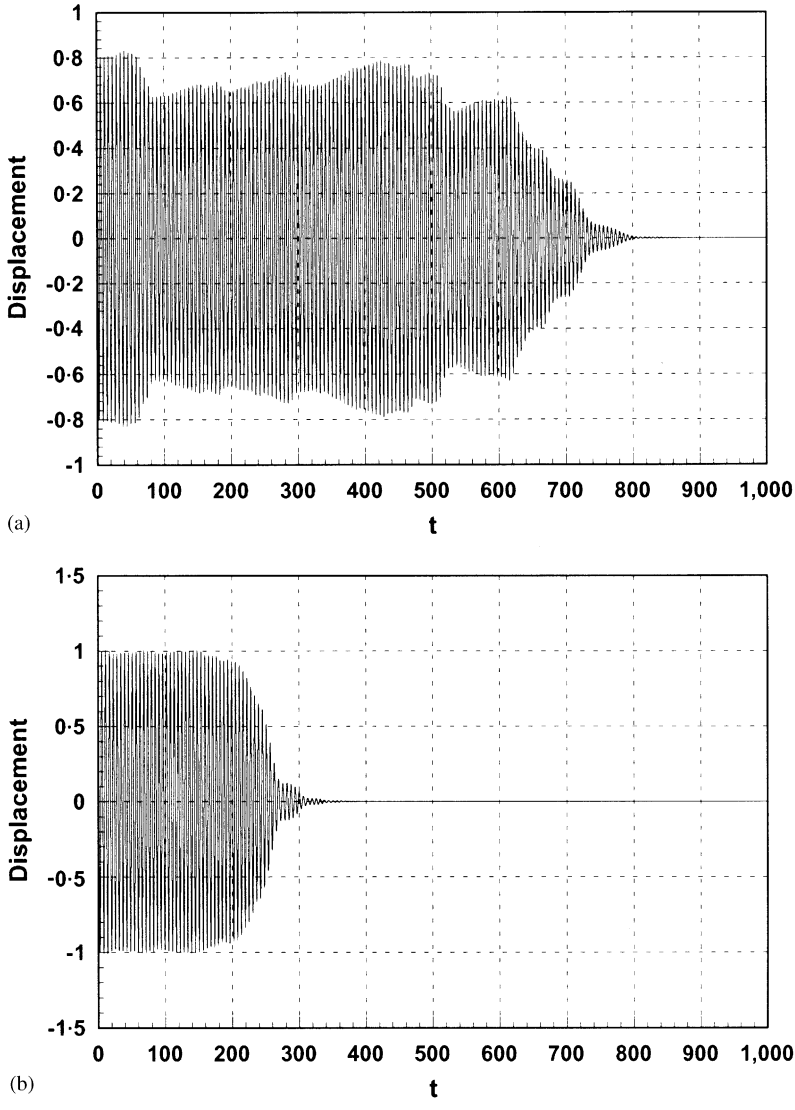

Figure 15. Sample function of displacement of system (46), $\alpha = 0{\cdot}3$, $\beta = 0{\cdot}09$, $\omega = 1{\cdot}0$, $E = 0{\cdot}2$: (a) $\Omega = 2{\cdot}1$, $\sigma^2 = 0{\cdot}01$; (b) $\Omega = 2{\cdot}2$, $\sigma^2 = 0{\cdot}01$; (c) $\Omega = 2{\cdot}3$, $\sigma^2 = 0{\cdot}01$; (d) $\Omega = 2{\cdot}1$, $\sigma^2 = 0{\cdot}05$.

5. CONCLUSION

In the present paper a stochastic averaging procedure for strongly non-linear oscillators subject to external and/or parametric excitation of bounded noise has been developed. By using the stochastic averaging method, the primary resonance of Duffing oscillator with hardening spring under external excitation of bounded noise has been studied. The stochastic jump and its bifurcation of the Duffing oscillator have been briefly examined by using the stationary joint probability density of amplitude and phase. Two major differences between the deterministic and stochastic jumps have been pointed out and explained. The primary parametric resonance of Duffing oscillator with hardening spring

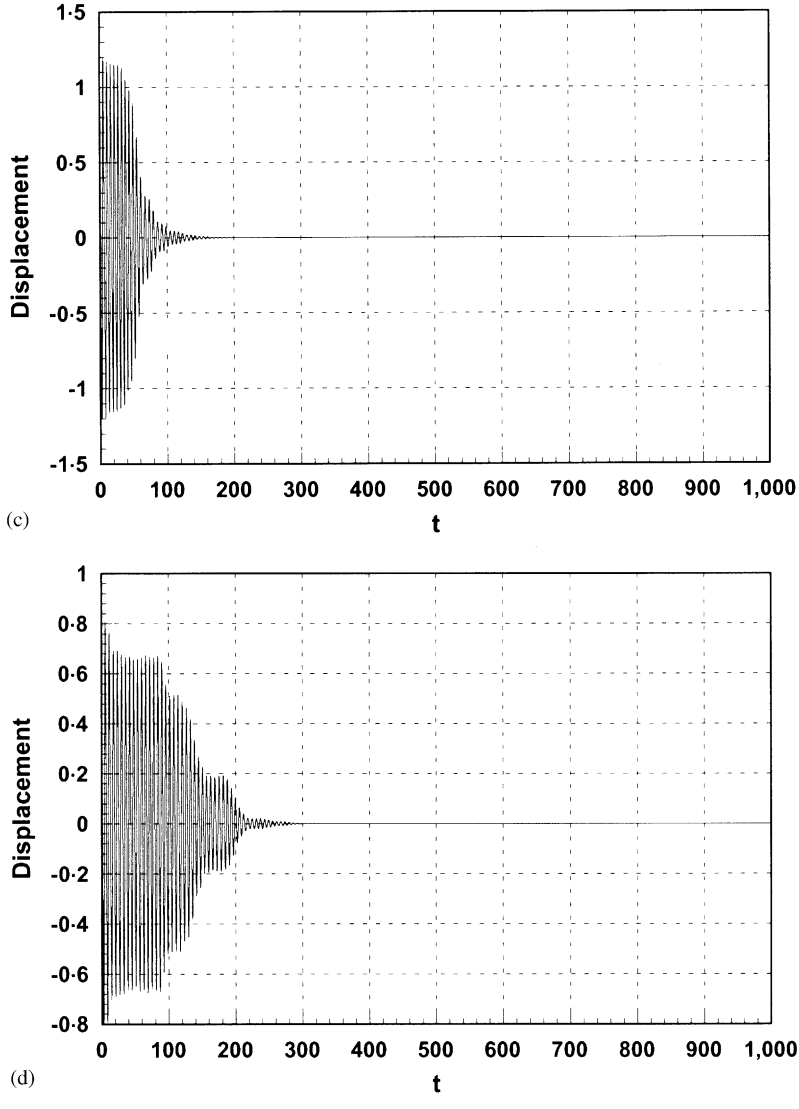

Figure 15. Continued.

under parametric excitation of bounded noise has also been examined by using the stochastic averaging method. The unstable region of the trivial solution of the oscillator has been delineated by evaluating the Lyapunov exponent of the linearized system. It has been observed that in the unstable region the stationary state of the system is a random vibration with non-zero amplitude while in the frequency interval of triple-valued amplitude solution, the system approaches equilibrium position without back jump, independent of the initial condition. The reason for this behaviour has been explained.

ACKNOWLEDGMENTS

The work reported in this paper was supported by the National Natural Science Foundation of China under Grant Nos. 19972059 and 10002015. The financial support

from the Hong Kong Polytechnic University through the Area of Strategic Development (ASD) Programme is also gratefully acknowledged.

REFERENCES

1. G. Q. Cai and Y. K. Lin 2001 *Nonlinear Dynamics* **24**, 3–15. Random vibration of strongly nonlinear systems.
2. W. Q. Zhu, Z. L. Huang and Y. Suzuk 2001 *International Journal of Non-linear Mechanics* **36**, 1235–1250. Response and stability of strongly non-linear oscillators under wide-band random excitation.
3. C. Sobiechowski and L. Socha 2000 *Journal of Sound and Vibration* **231**, 19–35. Statistical linearization of the Duffing oscillator under non-Gaussian external excitation.
4. R. H. Lyon, M. Heckl and C. B. Hazelgrove 1961 *Journal of the Acoustical Society of America* **33**, 1404–1411. Response of hard-spring oscillator to narrow-band excitation.
5. W. Q. Zhu, M. Q. Lu and Q. T. Wu 1993 *Journal of Sound and Vibration* **165**, 285–304. Stochastic jump and bifurcation of a Duffing oscillator under narrow-band excitation.
6. R. L. Stratonovich 1967 *Topics in the Theory of Random Noise*, Vol. 1. New York: Gordon and Breach.
7. M. F. Dimentberg 1988 *Statistical Dynamics of Nonlinear and Time-Varying Systems*. Taunton: Research Studies Press.
8. Y. K. Lin, Q. C. Li and T. C. Su 1993 *Journal of Wind Engineering and Industry Aerodynamics* **49**, 507–516. Application of a new wind turbulence model in predicting motion stability of wind-excited long-span bridges.
9. S. T. Ariaratnam 1996 in *Advances in Nonlinear Stochastic Methods*, *Proceedings of IUTAM Symposium* (A. Naess and S. Krenk, editors) 11–18. Dordrecht: Kluwer Academic Publishers. Stochastic stability of viscoelastic systems under bounded noise excitation.
10. W. Y. Liu, W. Q. Zhu and Z. L. Huang 2001 *Chaos, Solitons and Fractals* **12**, 527–537. Effect of bounded noise on chaotic motion of Duffing oscillators under parametric excitations.
11. Z. L. Huang, W. Q. Zhu and Y. Suzuki 2000 *Journal of Sound and Vibration* **238**, 233–256. Stochastic averaging of strongly non-linear oscillators under combined harmonic and white noise excitations.
12. Z. Xu and Y. K. Cheung 1994 *Journal of Sound and Vibration* **174**, 563–576. Averaging method using generalized harmonic functions for strongly non-linear oscillators.
13. P. E. Kloeden and E. Platen 1992 *Numerical Solution of Stochastic Differential Equations*. Berlin: Springer-Verlag.
14. A. Naess and V. Moe 1998 in *Structural Safety and Reliability* (M. Shinozuka and Y. K. Wen, editors), 795–801. Rotterdam: Balkema. New techniques for path integral solution of random vibration of nonlinear oscillators.
15. B. N. Sun, Z. G. Wang, J. M. Ko and Y. Q. Ni 2000 in *Advances in Structural Dynamics* (J. M. Ko and Y. L. Xu, editors), Vol. 1, 553–560. Amsterdam: Elsevier. Cable oscillation induced by parametric excitation in cable-stayed bridges.
16. N. N. Bogoliubov and Y. A. Mitropolsky 1961 *Asymptotic Methods in the Theory of Nonlinear Oscillators*. New York: Gordon and Breach.